American Mineralogist, Volume 67, pages 749–761, 1982

The colors of sillimanite

GEORGE R. ROSSMAN

Division of Geological and Planetary Sciences
California Institute of Technology
Pasadena, California 91125[1]

EDWARD S. GREW AND W. A. DOLLASE

Department of Earth and Space Sciences
University of California
Los Angeles, California 90024

Abstract

Sillimanite occurs in three colored varieties: yellow, brown, and blue. The yellow color is characteristic of unaltered single crystals of sillimanite from high-grade metamorphic rocks and associated pegmatites. Such sillimanites contain up to 1.8 wt.% Fe_2O_3 and up to 0.3% Cr_2O_3. The yellow color is due to Fe^{3+}, or in a few cases, to Cr^{3+}. The ion dominant in the optical spectrum of sillimanite containing negligible Cr^{3+} is Fe^{3+} in tetrahedral coordination. However, Mössbauer data suggest that about 80% of the iron is in octahedral coordination and only 20% in tetrahedral coordination. The salient features in the optical spectrum from Fe^{3+} are absorption bands at 462, 440, and 412 nm in α, 616, 474, and 438 nm in γ, and 361 nm in α and γ. No evidence for Fe^{2+} was found. Absorption from Cr^{3+} occurs near 620 and 423 nm. The brown variety is also formed in high-grade metamorphic rocks and associated pegmatites; some brown sillimanite is chatoyant from abundant acicular inclusions oriented parallel to c. Brown sillimanite generally contains 1 or more wt.% Fe_2O_3. Optical absorption spectra of brown sillimanite include some of the iron features characteristic of yellow sillimanite and prominent bands at ~452 nm and 542 nm. These last two bands may be due to incipient exsolution of an iron-rich phase, which appears to constitute the inclusions. Blue sillimanite has been documented from crustal xenoliths in basalt at two localities and from alluvial deposits at two other localities. Blue sillimanite contains no more than 1 wt.% Fe_2O_3. The prominent absorption features, restricted to γ, consist of two bands at 595 and ~836 nm. The spectra are similar to those of blue kyanite. As with kyanite, it is likely that the coloration is the result of intervalence charge transfer although the intensity of the absorption bands is not correlated with either Fe or Ti content.

Introduction

Sillimanite, Al_2SiO_5, occurs in three principal colored varieties—yellow, brown, and blue. The yellow and brown varieties are widespread whereas the blue variety is a mineralogical curiosity that has been well-documented from only four localities worldwide. Iron, chromium and titanium are the most abundant minor elements in sillimanite and the most likely to be responsible for the color. Grew and Rossman (1976a, b) and Grew (1976) had previously communicated the results of a study of the optical absorption of a blue and a yellow sillimanite and observed that the absorption spectra of these varieties are fundamentally different. They suggested that the yellow color is largely due to Fe^{3+} in tetrahedral coordination. On the other hand, Hålenius (1979) reported an absorption spectrum of a yellow sillimanite and concluded that iron in the six-coordinate site was responsible for the color.

In a study of the electron paramagnetic resonance of Oconee County, South Carolina, sillimanite, Le Marshall *et al.* (1971) observed signals from two crystallographically inequivalent Fe^{3+} ions and

[1]Contribution No. 3665

0003–004X/82/0708–0749$02.00

based the interpretation of their data on the assumption that Fe^{3+} occurred in both the six-coordinate and four-coordinate sites. The present study, an extension of our earlier work, attempts to provide a systematic examination of a number of sillimanites which span the range of color variation. It is the purpose of this study to examine the origin of these colors, and to relate the colors to the petrologic environment in which sillimanite forms.

Methods

Samples of sillimanite for this study were selected from (1) granulite-facies rocks collected in Antarctica, (2) crustal xenoliths collected at Kilbourne Hole, New Mexico, U.S.A. and Bournac, Haute-Loire, France, and from (3) specimens obtained from museum and private collections (Tables 1–3).

Compositions of sillimanite were determined on carbon coated thin sections and isolated grains at the electron microprobe facilities at UCLA and Caltech. The average, maximum, and minimum values for Fe_2O_3 for each sample (Tables 1 and 3) are based on analyses at four to six points on three to six grains in each thin section of the sillimanite-bearing rock (sample 15, Table 3, consists of two grains broken from one piece). The TiO_2 contents of samples 14 and 19 are based on an analysis at one point per sample. The tabulated analyses are averages of both referenced literature analyses and new data. Optical spectra were obtained using methods described by Rossman (1975). ε-Values are in units of liters per mole per cm. The intensities presented in Figure 2 were obtained by constructing a line tangent to local minima on the sides of the absorption band. There are consequently uncertainties associated with the values obtained for bands which were shoulders on steeply rising baselines, such as the bands at 390 nm and 361 nm in α and at 361 nm in γ. Mössbauer spectra were obtained on about 210 mg of acid-washed hand-picked grains. The sample densities were about 0.012 mg ^{57}Fe per cm^2. Isomer shifts are reported relative to iron in Pd.

Yellow sillimanite

Mode of occurrence and composition

We have analyzed samples of yellow sillimanite from six localities (Table 1). Samples 1, 2, and 4 are from granulite-facies rocks in Antarctica and the Adirondack Mountains, New York (Grew, 1980, 1981a). The sillimanite in samples 1 and 2 is associated with ilmenite, and that in 4, with magnetite.

Table 1. Chemical composition and localities of yellow-green sillimanite

Sample		1	2	3	4	5	6
Al_2O_3		-	62.21	61.46	61.74	60.84	62.17
SiO_2		-	36.19	-	36.77	36.52	37.19
Fe_2O_3	Max	1.33	0.85	1.87	1.97	0.69	-
	Ave	1.28	0.85	1.78	1.79	0.62	1.41
	Min	1.22	0.84	1.63	1.70	0.56	-
TiO_2		0.01	0.02	0.03	0.02	0.02	0.02
Cr_2O_3		0.003**	0.21*	0.08	0.00	0.15†	0.00
Number of points (probe analyses)		10	4	8	9	3	-

1. Reinbolt Hills, Antarctica (70°28'S, 72°27'E). Grew #556 and NMNH 137011. From pegmatite in granulite-facies rocks.
2. Molodezhnaya Station, Antarctica (67°40'S, 45°50'E). Grew #274B. From garnet-biotite quartzofeldspathic gneiss. Analysis: Grew (1980).
3. Kilbourne Hole, New Mexico, U.S.A. Grew #76-5-1. From crustal xenolith in core of basaltic bomb. Analysis: Grew (1980).
4. Benson Mines, New York, U.S.A. NMNH 115586. From magnetite-quartz-sillimanite iron-ore. Analysis: Grew (1980).
5. Forefinger Point, Antarctica (67°37'S, 48°04'E). Grew #2113. From coarse-grained sillimanite-orthopyroxene-cordierite-biotite ± sapphirine rock.
6. Brevig, Norway. Analysis: Hålenius (1979).

Table entries in weight percent.
Analyses are electron microprobe, except:
* Energy dispersive analysis on scanning electron microscope (EDA)
** Emission spectrographic analysis (ESA). Also by ESA on number 1: 0.006% Be and 0.005% V.
† X-ray fluorescence analysis: 0.01% V; Mn absent.
Abbreviations: NMNH: National Museum of Natural History, Smithsonian Institution.

Sample 1 is part of a cm-sized single crystal from a subconcordant garnetiferous pegmatite lens in garnet biotite quartzofeldspathic gneiss. Fe_2O_3 contents of the pegmatitic sillimanite from this locality vary from crystal to crystal (0.76 to 1.30 wt.% Fe_2O_3, Grew, 1980) and the Fe_2O_3 contents in Table 1 were obtained on the piece used in the optical absorption work.

Sample 5 is from granulite-facies rocks of the Archean Napier complex at Forefinger Point in the western part of Casey Bay, Enderby Land, Antarctica (Grew and Manton, 1979; *cf.* sample 12 of brown sillimanite, below). It was collected from a layer 1.5 m thick of aluminous granulite containing orthopyroxene, sillimanite, cordierite, biotite, and sapphirine; other rock types present at Forefinger Point are pyroxene–hornblende granulite, garnet–quartz–feldspar gneiss, and charnockitic gneiss. Sillimanite in sample 6 from Brevig, Norway, is associated with quartz, K-feldspar, biotite, hematite and magnetite (Hålenius, 1979). Samples 1, 2, 4, 5, and 6 are representative of prismatic, Fe_2O_3-bearing, sillimanite that is found in many high-grade metamorphic terrains.

Sample 3 is from a sillimanite–quartz–K-feld-

spar–ilmenite–magnetite gneiss xenolith containing abundant glass, which was found among the ejecta at Kilbourne Hole maar, New Mexico (Grew, 1979, 1980). Xenoliths of quartzofeldspathic gneiss such as sample 3 and the samples containing blue sillimanite (see below) may be derived from a granulite-facies complex in the lower third of the earth's crust under Kilbourne Hole (Padovani and Carter, 1977a). During their incorporation in the basalt host and transport to the earth's surface, the xenoliths have been partially fused either by heating or decompression, and subsequently quenched (Padovani and Carter, 1977b; Grew, 1979).

Optical spectra

Millimeter thick plates of sample 1 have the pleochroic formula, X = yellow, Y = green-yellow, and Z = colorless. Its optical absorption spectrum (Fig. 1) is representative of yellow sillimanites except sample 5. The spectrum is rich in structure; salient features are absorption bands at 462, 440, and 412 nm in α and 616, 474, and 438 nm in γ, and an additional band at 361 nm, prominent in α and γ, but off scale in Figure 1. Bands in the 700 to 900 nm region are weak or absent. An absorption feature is present at 1027 nm in the α and γ spectra of all thick samples examined. Its width is much narrower than iron features which occur in this region in the spectra of other minerals. Because its intensity is proportional to the thickness of the sample but not proportional to iron content, it is tentatively ascribed to a vibrational overtone of sillimanite. The depth of color and the intensities of all other absorption bands, except the 616 nm γ band (the dominant cause of absorption in the 620 nm region), generally increase with iron content (Fig. 2). Consequently, we attribute all the absorption bands except 616 nm to iron. The absorption of sample 3 is anomalously low at most wavelengths. We doubt if this is due to compositional inhomogeneity because it was observed in multiple optical and chemical analyses of fragments of sample 3.

The intensity of the ~616 nm γ band varies among the different samples. The band is less intense relative to the other features in the spectrum of sample 4 (Fig. 3). Although its intensity is not correlated with iron content, its intensity behavior in Fig. 2 suggests that it still could be related to iron. In sample 3, where the iron absorption bands, notably the 361 nm (γ) band, have intensity below the general trend, the 616 nm band is prominent. A possible interpretation of this behavior is that the 616 nm band represents iron in a different environment in sillimanite. The origin of this band has yet to be established. This band imparts a greenish tint to the otherwise yellow crystals. Chromium also causes absorption in this region, which we will discuss below.

Stoichiometry (Grew, 1980), Mössbauer spectra (see below), absorption band positions and intensities indicate that the oxidation state of iron is +3. The intensities of the prominent absorptions expressed as absorption coefficients (ε-values), calculated for sample #1 under the assumption that all of

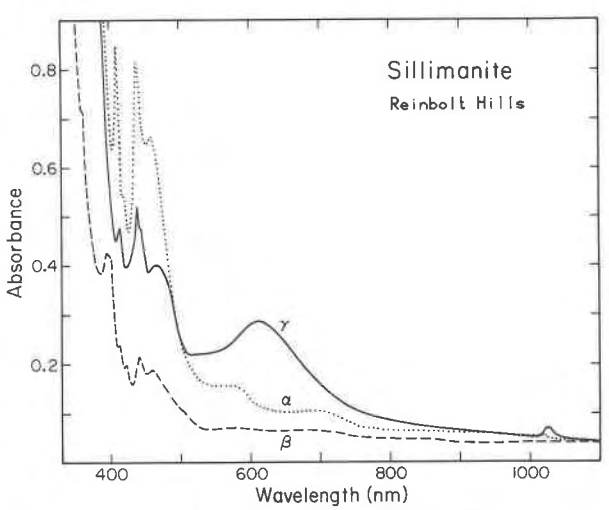

Fig. 1. Optical absorption spectrum of yellow sillimanite from Reinbolt Hills (#1). Thickness: 5.0 mm, E$\|a = \alpha$ = dots; E$\|b = \beta$ = dash; E$\|c = \gamma$ = solid line.

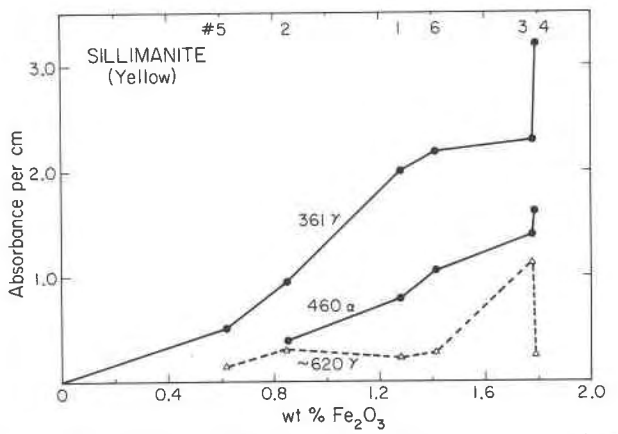

Fig. 2. Correlation of the intensities of the optical absorption bands of yellow sillimanites with average Fe_2O_3 concentration. Bands at 361, 390, 410, and 440 nm in α and at 390, 410, and 440 nm in γ follow trends which generally parallel these illustrated for 361 nm (γ) and 460 (nm (α). Absorption in the 620 nm region includes both the 616 nm and and the Cr^{3+} bands.

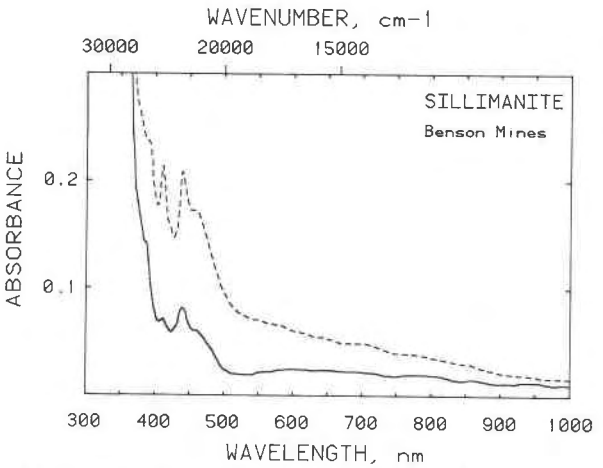

Fig. 3. Optical absorption spectrum of yellow sillimanite from Benson Mines (#4), showing the near absence of the 620 nm band. Thickness; 400 μm; α = broken line; γ = solid line.

the iron contributes to each peak, are: 412 nm (α) $\varepsilon = 3.9$; 449 nm (α) $\varepsilon = 3.0$; 361 nm (γ) $\varepsilon \sim 3.8$. These intensities, low for most metal ions in crystals are consistent for spin forbidden Fe^{3+} transitions. If the Fe^{3+} were present in more than one site, these ε-values would be lower limits for one of the sites.

Absorption features of Fe^{2+} are expected in the 800–1200 nm region with an ε greater than 3. From the intensity of the absorption of sample #1 in the 850 nm region in the β spectrum, an upper limit for the Fe^{2+} content can be calculated assuming $\varepsilon = 3$. At most, the Fe^{2+} content could be 0.012%, FeO corresponding to 0.9% of the total iron. The absorption features at 826 and 1205 nm reported by Hålenius (1979) and associated with Fe^{2+} were not observed in any of our spectra, including that of his sample (#6).

Assignment of the Fe^{3+} to a particular site in the crystal structure of sillimanite is more difficult. Both a tetrahedral and an octahedral Al site (Burnham, 1963a) are available for Fe^{3+} substitution. The complexity of the spectrum suggests Fe^{3+} substitution on both sites. Moreover, the spectrum differs from the patterns for minerals containing Fe^{3+} in only octahedral coordination, such as green kyanite, andradite, and chrysoberyl. Kyanite is an ideal comparison standard because aluminum occupies only sites of six coordination with average Al–O bond distances comparable to those of sillimanite (Burnham, 1963b). Stoichiometry, electron spin resonance data (Hutton and Troup, 1964), and optical spectra indicate that trivalent cations, including Fe^{3+}, substitute in the aluminum sites. The absorption pattern of Fe^{3+} in kyanite consists of broad bands at 1075 (0.35) and 610 nm (0.6) and pairs of sharp bands at 444 and 437 nm (1.6) and 377 and 370 nm (~3.5) (White and White, 1967; Faye and Nickel, 1969). The ε values, which we determined for a Brazilian kyanite, follow the wavelengths in parentheses. The 1075 nm band occurs at an energy unusually low for Fe^{3+}, a direct consequence of the substitution of Fe^{3+} into an Al^{3+} site of smaller average metal-oxygen bond distance than is normally found for Fe^{3+}. The absence of such a band at lower energy in the sillimanite spectrum indicates the absence of a major spectroscopic contribution from Fe^{3+} in the six-coordinate site. However, the low intensity of Fe^{3+} in the 1075 nm region of kyanite means that in the spectrum of sillimanite #1, nearly 0.7 wt.% octahedral Fe^{3+} would have to be present to be reliably detected by a band in the 1000 nm region. If this much octahedral Fe^{3+} were present, the kyanite spectral model predicts that the contribution from octahedral Fe^{3+} would only be as intense as the β spectrum in Figure 1. Because the sillimanite α and γ spectra are much more intense than the β spectrum, the more intense features in the sillimanite spectrum are not due to octahedral Fe^{3+}.

Experimental spectroscopic standards for tetrahedral Fe^{3+} are less well established than those for octahedral Fe^{3+}. Orthoclase: Fe^{3+} (Faye, 1969) and $AlPO_4$: Fe^{3+} (Lehmann, 1970) are relevant standards because they contain low concentrations of Fe^{3+} in a tetrahedral site and have spectra which have several similarities to the sillimanite spectra. Because the positions of the stronger absorption bands in the 350–500 nm region are in the same range as those of octahedral Fe^{3+}, site occupancy cannot be readily determined by a wavelength criterion. The ε values of tetrahedral Fe^{3+} bands in the 300–500 nm region can be as much as an order of magnitude higher than those of octahedral Fe^{3+}. The intensity of the sillimanite pattern can be explained if a portion of the iron is in the tetrahedral site.

Consequently, we propose that: (1) the more intense features in α and γ are due to Fe^{3+} in the tetrahedral site; (2) the weaker features could be due to Fe^{3+} in either the octahedral site or the tetrahedral site; (3) tetrahedral Fe^{3+} is the spectroscopically dominant ion and primary cause of the color in the crystal; and (4) even if most of the iron in sillimanite were in octahedral coordination, its contribution to the color would be minor.

Mössbauer spectral analysis

Mössbauer spectra are consistent with the presence of Fe^{3+} in two sites. Spectra were obtained on the two samples richest in iron, numbers 3 and 4. Although a long counting time was employed, with background counts of over 6×10^6 counts per channel, the spectrum (Fig. 4) of sample #4 is weak due to its low iron content. It consists of two main lines; a more intense lower velocity peak and a less intense high velocity peak. When a doublet constrained to have equal area lines but independent linewidths is matched to this spectrum, a statistically satisfactory fit is obtained (rms chi value 1.09). The asymmetric doublet would have an isomer shift (I.S.) of 0.18 mm/sec and a quadrupole splitting (Q.S.) of 1.04 mm/sec. The higher velocity, broader peak has an apparent width of 0.81 mm/sec and the lower velocity peak is narrower with an apparent width of 0.58 mm/sec. The isomer shift is somewhat low but not inconsistent with octahedrally coordinated ferric iron. The quadrupole splitting is a little higher than usually observed in such compounds. The apparent line widths and asymmetry would be anomalous for a high-iron content mineral, but could be rationalized as due to relaxation broadening (Wignall, 1966) brought about by the long Fe–Fe distances in such a low-iron content phase.

There are several sources of dissatisfaction with this fit. The two-line fit does not account for an anomalous absorption area between the two fitted peaks and the correspondence in shape between the observed and fitted peaks is poor. The observed peaks both seem to be more intense and narrower than their best-fit approximations. Because the appearance of the two-peak fit suggests that a second, weaker doublet was present, a two doublet fit was attempted. With two-doublets, the fit is improved (rms chi = 1.02), but this improvement is not significant compared to the large statistical uncertainty present in this weak spectrum. The two-doublet fit is reported because it is both consistent with the observed spectrum and is thought to lead to an interpretation which is more realistic in view of the known crystal chemistry of sillimanite.

In order to minimize the number of fitted variables and ensure convergence of the fit, the doublets were constrained to be symmetric, *i.e.*, each half having the same area, and all four peaks having the same width. In addition, as the low velocity peaks of each doublet are essentially completely overlapped, the location of the weaker low-velocity peak was held fixed at the location of the envelope maximum. As a result of applying these constraints, the two-doublet fit has only one more free variable than the one-doublet fit.

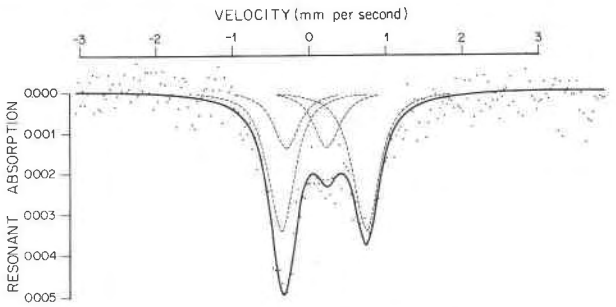

Fig. 4. Mössbauer spectrum of yellow sillimanite from Benson Mines (#4) fitted with two constrained doublets. Velocities are given in mm/sec relative to Fe in Pd. Absorbance is given as the fraction of the background count.

The constrained two-doublet fit (Fig. 4) converged yielding the following parameters:

outer doublet: 79(±5)% of area,
I.S. = 0.19(±.02) mm/sec,
Q.S. = 1.11 (±.03) mm/sec.

inner doublet: 21(±5)% of area,
I.S. = −0.03(±0.5) mm/sec,
Q.S. = 0.53(±−1) mm/sec.

The major doublet in either the one or two-doublet fit has an isomer shift appropriate for Fe^{3+} in octahedral coordination. In analogous minerals, ferric ions in octahedral sites give I.S. values of about 0.20±.03 mm/sec. The weaker inner doublet of the two-doublet fit has a smaller isomer shift of *ca.* −0.03 mm/sec, which is in the range expected for ferric iron in tetrahedral coordination. Analogous silicates and oxides with tetrahedrally coordinated ferric ions give I.S. values of *ca.* 0.01±.05 mm/sec.

The quadrupole splitting of ferric doublets generally increases with increasing distortion of the Fe site. The Q.S. of the major, or octahedral, doublet, at *ca.* 1.1 mm/sec is moderately large suggesting a moderately distorted site. For comparison, octahedral Fe^{3+} in pyroxenes, garnets, amphiboles and micas give Q.S. values of about 0.4 to 0.6 mm/sec, and in such very distorted sites as the M(3) site in epidote, the Q.S. is 2.0 mm/sec or higher. The Q.S. of the weaker, or tetrahedral, doublet is smaller. However, it is difficult to assess the significance of this value, as the Q.S. values reported for the few tetrahedrally coordinated cases studied range from

near zero for some spinels to about 1.5 mm/sec for some pyroxenes.

The fitted linewidth in the two-doublet case, 0.44(±.02) mm/sec, is significantly narrower and probably closer to reality than those given by the one-doublet fit. However, the true linewidths are probably all unequal considering the low iron content of this mineral. Meaningful refinement of separate linewidths is precluded by the quality of the spectrum.

The Mössbauer spectrum of sample 3 is too weak and ill-defined to be of quantitative value. This spectrum (two mirror image halves) was recorded over 1024 channels with a velocity increment of 0.02 mm/sec-channel. A background count of 2.45 $\times$ 10^6 counts per channel was accumulated. The maximum dip was only 0.003 of background and the Ruby "S" parameter which is a measure of the information content of the spectrum, is only about 1/3rd the value of the spectrum of sample 4. A one-doublet fit results in Mössbauer parameters that agree with those of sample 4 within the large experimental error. There is no indication of ferrous iron. The low quality of this spectrum precludes fitting separate octahedral and tetrahedral doublets.

It is not apparent why sample 3 shows distinctly lower resonant absorption. The optical absorption features we attribute to iron, except the 616 nm γ band, are also anomalously low in this sample (see above). This may possibly reflect a more homogeneous iron atom distribution resulting in more isolated iron atoms and therefore more severe relaxational broadening of the Mössbauer spectrum. A more random distribution of iron in this sillimanite from Kilbourne Hole is also suggested by the highly disordered Al–Si distribution in K-feldspar of the Kilbourne Hole xenoliths (Grew, 1979).

During the course of this study Hålenius (1979) published Mössbauer spectra of a sillimanite from Benson Mines, New York, the same locality as that for sample #4, and of a Norwegian sillimanite (#6) whose optical spectra we have also studied. His spectra not only show greater dips and smaller statistical noise than ours, which is consistent with his use of a stronger source and thicker samples, but also his conclusions differ from ours. Hålenius fitted his sillimanite spectra with three symmetrical doublets with the strongest feature being a Fe^{3+} doublet at I.S. = 0.19(1), Q.S. = 1.07(1) and linewidth = 0.63(1) mm/sec. These values are essentially identical with the octahedral Fe^{3+} doublet we observed except for the broadened linewidth. The remaining doublets have been assigned by Hålenius to an Fe^{2+} component in sillimanite and a hematite impurity phase present in his sample. The Brevig, Norway, sillimanite in particular had a prominent Fe^{2+} component in its Mössbauer spectrum (Hålenius, 1979). However, we observed no prominent Fe^{2+} features in the optical spectra of his Brevig, Norway, sample, and Fe^{2+} or hematite features could not be detected in our Mössbauer spectra. The Fe^{2+} features in Hålenius' spectra may be due to another contaminant phase. These contaminant phases are not observable in our sillimanite samples, which were carefully picked free of visible impurities by hand.

The conclusions from our combined Mössbauer and optical spectra are: (1) iron in yellow sillimanite occurs in the ferric oxidation state: (2) about 4/5ths of this ferric iron is in octahedral sites; (3) the remaining 1/5th is in tetrahedral coordination—no doubt substituting for the trivalent aluminum present on both these sites; (4) the yellow color is primarily caused by the tetrahedral Fe^{3+}; (5) the 616 nm band, when present, imparts a green component to the yellow color; (6) the prominent absorption bands in the spectrum of yellow sillimanite are present in the spectra of nearly all sillimanites including these for brown and blue sillimanite discussed below.

Heating experiments

To determine whether the proposed dual octahedral–tetrahedral Fe^{3+} occupancy is temperature dependent, samples 1, 3 and 4 were heated under various conditions at temperatures from 500 to 1430° C for up to 130 hours under air, charcoal and $fO_2 = 10^{-10}$. Essentially no changes in the color or spectra occurred up to 1050° C. In the 1430° C experiment, sample 1 lost the trace OH^- evident in the infrared spectrum, became translucent, but showed essentially no change in the Fe^{3+} spectrum.

Other cations

Chromium is an important minor element in samples 2 and 5. In the spectrum of sample 5, absorption bands not due to Fe^{3+} occur at ~620, 523 and 423 nm (Fig. 5). The bands at 620 and 423 nm are at wavelengths similar to those from the spectrum of Cr^{3+} in emerald which is in a six-coordinated site. Their approximate ε values in γ based on Cr^{3+} are: 620 nm $\varepsilon = 5$; and 423 nm $\varepsilon = 15$. The cause of the 523 nm band has not been established.

Brown sillimanite

Mode of occurrence and composition

We examined samples of brown sillimanite from seven localities (Table 2). Six of the sillimanites are from quartz veins, and the seventh, from a pegmatite. The prisms of brown sillimanite we examined range from less than 1 mm to over 3 cm in width.

The sillimanite-bearing quartz most likely occurs as veins in mica schist or gneiss. The sillimanite is associated with ilmenite, a hematite–ilmenite intergrowth, or rutile, as well as biotite, muscovite, or minor secondary sericite. Sample 10 from Oconee County, South Carolina, is a loose crystal. In F. H. Pough's samples from this locality, brown sillimanite occurs with ilmenite, biotite and muscovite in quartz. This paragenesis is the same as that of sillimanite from the type locality in Saybrook, Connecticut (Bowen, 1824). Although our samples appear to be found only in quartz, sillimanite at Norwich (presumably also brown) also occurs in mica schist (Schairer, 1931, p. 112).

The Connecticut localities are in the sillimanite and sillimanite–K-feldspar zones of regional metamorphism, roughly equivalent to the upper amphibolite facies and possibly the hornblende granulite facies (Thompson and Norton, 1968). The Oconee County sillimanite is most likely derived from amphibolite facies metamorphic rocks, which underlie this part of South Carolina (Overstreet and Bell, 1965). As we have no information on the exact locality for the Sardinian sample, we do not know the grade of metamorphism of the source terrain for this sample.

The pegmatitic sillimanite (#12) is from "Christmas Point" (informal name), a part of an unnamed island near McIntrye Island in the eastern part of Casey Bay, Enderby Land, Antarctica. This pegmatite cuts granulite-facies rocks of the Archean Napier complex, the same complex from which the Forefinger Point sillimanite (#5) originated. Coarse-grained portions of the pegmatite consist largely of quartz, microcline (in part red), biotite, apatite and sillimanite; and medium-grained portions of surinamite, cordierite, garnet, apatite, pyrite, orthopyroxene, wagnerite, ilmeno-hematite, and sillimanite (Grew, 1981b). Sillimanite, some of which is dark brown and chatoyant, forms single crystals up to 10 cm long and 3 cm across. This pegmatite and the enclosing granulite-facies rocks constitute a block of relatively unaltered rock in a tectonic zone (possibly of early Paleozoic age) of intense deformation, retrogression of the granulite-facies rocks under amphibolite facies conditions, and of emplacement of pegmatite veins. In general, chatoyancy and brown color are characteristic of some sillimanites in relatively unaltered masses of rock exposed in Casey Bay and intersected by these tectonic zones. Away from these zones, Enderby Land sillimanite is gray, white, or pale yellow (*e.g.*, #5, Forefinger Point).

In addition to the above examples, patches pleochroic in brown (maximum absorption $\|c$) have been reported in thin sections of sillimanite in granulite from Wilson Lake, Labrador, Canada (Leong and Moore, 1972, p. 787; Grew, 1980). This sillimanite is associated with magnetite and titaniferous hematite, plagioclase, biotite, sapphirine, and orthopyroxene. Metamorphism was under conditions of the granulite-facies (Leong and Moore, 1972; Morse and Talley, 1971). Vrána (1979, p. 26) reports "patches of light brown coloration . . .

Table 2. Fe_2O_3 contents and localities for brown sillimanite

Sample	7	8	9	10	11	12	13
Fe_2O_3	1.02	1.20	1.12	1.33	0.98	1.35	1.30

Table entries in weight percent, by energy dispersive analyses.
7. Willimantic, Connecticut, U.S.A. NMNH C3019-2. With hematite-ilmenite and rare biotite in quartz.
8. Vernon, Connecticut, U.S.A. NMNH B14835. With biotite, rutile, and hemo-ilmenite in quartz.
9. Guilford(?), Connecticut, U.S.A. Harvard Univ. Coll. 85919. In quartz.
10. Oconee County, South Carolina, U.S.A. NMNH R11616.
11. Sardinia(?). NMNH R3741. In quartz.
12. "Christmas Point", on an unnamed island 5 km WSW of McIntyre Island (67° 22'S, 49° 05'W), Antarctica, Grew #2292D. In pegmatite.
13. Norwich, Connecticut, U.S.A. Harvard Univ. Coll. 85918. With biotite, ilmenite, and minor muscovite in quartz.

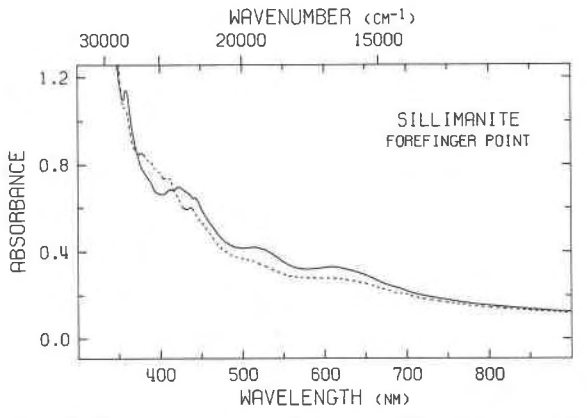

Fig. 5. Optical spectrum of yellow sillimanite containing chromium from Forefinger Point (#5). Thickness = 3.0 mm; α = broken line, γ = solid line.

passing in their centers into areas of opaque dusty particles" in sillimanite in a borosilicate rock containing magnetite and hemo-ilmenite from Zambia.

Brown sillimanite we have examined typically has numerous fine acicular inclusions, most of which are oriented parallel to [001]. Viewed down [001] brown sillimanite appears pale blue because of scattering from these inclusions; these inclusions cause the chatoyancy noted in some of our samples. The brown color is not evenly distributed in the crystal, and is typically most intense in patches where the inclusions are most numerous. The inclusions are either opaque or are translucent and brown; some have a hexagonal outline in a view perpendicular to [001]. The brown inclusions may be hematite; the opaque inclusions may be ilmenite, magnetite, or some other iron-rich oxide mineral.

Brown sillimanite analyzed in this study does not contain significantly less than 1 weight percent Fe_2O_3 (Table 2); the Wilson Lake material contains 1.6 to 1.8 wt.% (Grew, 1980). Vrána (1979) reports 1.2 wt.% Fe_2O_3 in the colorless portions of crystals having brown patches. Thus the brown color appears only to develop in sillimanite containing at least 1 wt.% Fe_2O_3.

Optical spectra

The pleochroic formula in our samples is : X and Y = colorless to pale yellow in thin section (30 μm) and orange-brown in thick sections (0.1 mm) and Z = violet brown (see also Dana, 1920, p. 498; Winchell and Winchell, 1951, p. 520).

The spectrum of sample 11 (Fig. 6) is representative of brown sillimanite. The broad region of absorption in the γ spectrum extending throughout the visible portion of the spectrum displays two maxima corresponding to absorption bands at ~452 and 542 nm. The 361 nm (γ) sharp Fe^{3+} absorption band characteristic of the pattern of yellow sillimanites and weaker Fe^{3+} features in α and β, are also present. Other absorption bands, in γ, at about 894 nm and about 730 nm appear to be present. The effects of scattering can be best observed in the β-spectrum obtained on a (001) slab where the apparent absorption rises in a broad band centered near 600 nm and decreases near 400 nm to preferentially transmit blue (Fig. 7). The inclusions responsible for this effect presumably have a dimension comparable to the wavelength of visible light. A background absorption, steadily rising toward shorter wave-lengths as a result of scattering from presumably larger inclusions is in many cases superimposed upon the absorption pattern (Fig. 8).

The dominant minor element is iron (Table 2). Based on total iron content, the ε value for the 452 nm band of sample 11 is 300. This value is too high to be caused solely by Fe^{3+}. An intervalence charge transfer transition is a likely cause of this absorption, and has been proposed to cause an intense absorption in the spectrum of andalusite. The optical spectrum of andalusite shows weak absorption from Fe^{3+} and a strong, dominant absorption band polarized parallel to [001] at 481 nm (Faye and Harris, 1969). The 481 nm band is reminiscent of the 452 nm and 542 nm absorption bands of sillimanite. Both the andalusite and sillimanite bands are in-

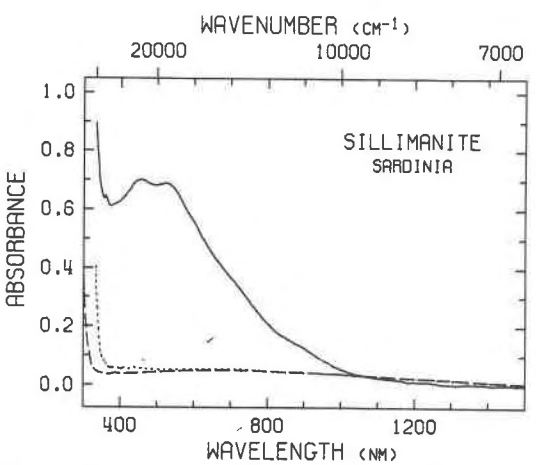

Fig. 6. Optical absorption spectrum of brown sillimanite from Sardinia(?) (#11) obtained with (100) and (010) slabs. 200 μm thick; α = dots, β = dash; γ = solid line. Data obtained in a region of the crystal chosen to minimize the contribution from scattering.

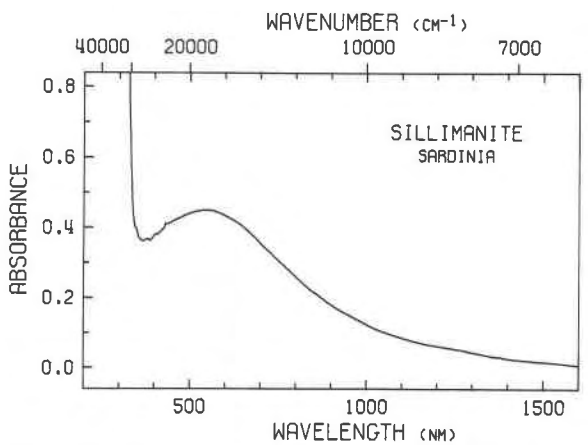

Fig. 7. Optical absorption spectrum of a (001) slab of brown sillimanite from Sardinia(?) (#11) obtained in a portion of the crystal which maximizes the spectral dependence of the scattering from the numerous inclusions oriented along [001]. Sample 237 μm thick; β polarization; the α polarization is nearly identical.

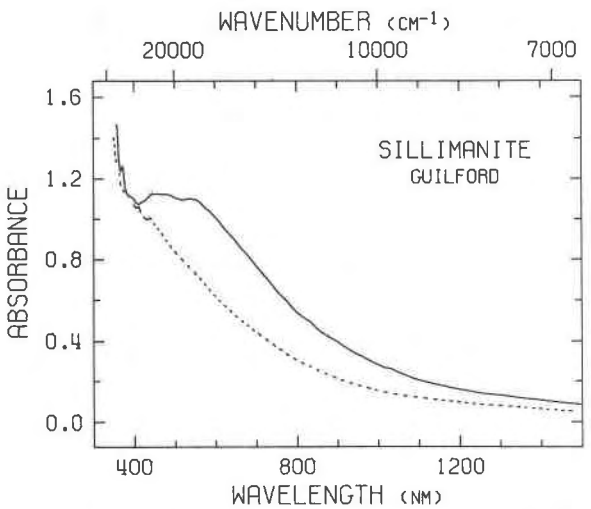

Fig. 8. Optical absorption spectrum of brown sillimanite from Guilford, Conn. (#9) showing the effects of background scattering. Thickness = 600 μm; α = broken line; γ = solid line.

tensely polarized parallel to the direction of the chain of edge-shared octahedra and have intensities much greater than can be accounted for by single-ion electronic transitions. Faye and Harris have proposed for andalusite a mechanism involving intervalence charge transfer betwen Ti^{3+} and Ti^{4+}. We do not consider an explanation involving Ti^{3+} to be likely for sillimanite in view of the relatively high Fe_2O_3 contents of brown sillimanite. Interactions involving Fe^{2+} such as Fe^{2+}/Ti^{4+} and Fe^{2+}/Fe^{3+} are more likely to be the cause. The absence of Fe^{2+} absorption indicates that if such mechanisms are operating, the amount of Fe^{2+} present is small. The association of the color with regions with inclusions suggests that the color originates from incipient exsolution. We propose that submicroscopic regions of an iron-rich phase in the process of exsolving are the source of the color. This suggestion is consistent with analytical electron microscopic observations that sillimanite #7 contains numerous small particles of titaniferous hematite ranging from 0.005 to 0.2 μm in dimension (David Veblen, personal communication, 1982).

Blue sillimanite

Mode of occurrence and composition

Samples of blue sillimanite available for study (Table 3) are gem quality single crystals up to 2 cm long from alluvial deposits at Mogok, Burma and in Sri Lanka (Spencer, 1920; Adams and Graham, 1926) and as prisms 0.1–5 mm long in xenolithic quartzofeldspathic gneisses at Kilbourne Hole, New Mexico, and Bournac, Haute-Loire, France (Caillère and Pobeguin, 1972; Padovani and Carter, 1973, 1974, 1977a; Grew, 1976, 1977a). Blue sillimanite has also been reported from Kenya (Bank, 1974) and from Davis Creek, New Zealand (Hattori, 1967). No details are available on the Kenya occurrence. Grew (1977b) found blue kyanite, but no blue sillimanite in the sample studied by Hattori (1967). The blue sillimanite reported in the New Zealand sample is possibly kyanite misidentified as sillimanite.

To our knowledge, there are no definitive reports of blue sillimanite *in situ* in Burma or Sri Lanka, and consequently, no data are available on its paragenesis. The Bournac paragenesis is similar to that at Kilbourne Hole (see above). Sillimanite-bearing xenoliths at Bournac may originate from the lower crust (Leyreloup *et al.*, 1977). By analogy with Kilbourne Hole, the Bournac xenoliths have probably also been subjected to decompression or heating by the basalt host during the xenolith's transport to the earth's surface. In contrast to the Kilbourne Hole xenoliths, however, glass and orthopyroxene-spinel intergrowths (replacing garnet) are much less abundant.

Sillimanite in eight xenoliths from Kilbourne Hole (including the 3 samples in Tables 1 and 3) and in 7 xenoliths from Bournac (including sample 19/20) were analyzed for iron (Grew, 1977a). The iron content, reported as Fe_2O_3, of blue sillimanite at

Table 3. Chemical composition and localities of blue sillimanite

		14	15	16	17	18	19	20	21	22
Al_2O_3		62.20	63.15	-	62.12	-	62.63	61.74	62.14	61.16
SiO_2		36.74	-	-	37.41	-	37.03	38.00	37.36	37.18
Fe_2O_3	Max	0.37	0.25	-	-	-	0.26	-	0.52	0.35
	Ave	0.36	0.25	-	0.32	-	0.21	0.17	0.46	0.35
	Min	0.35	0.24	-	-	-	0.18	-	0.41	0.35
TiO_2		0.04	0.01	-	0.02	-	0.02	0.09	0.08	0.05
Cr_2O_3		0.13*	-	-	0.10	-	0.00*	0.00*	0.02	0.05
Number of points		5	2	-	5	-	6[a]	1[b]	2	2

14. From xenolith of quartzofeldspathic gneiss, Kilbourne Hole, New Mexico, U.S.A. Grew #76-5 (collected by E. R. Padovani). Analysis: Grew (1980).
15. Mogok, Burma. Mus. Nat. d'Histoire Naturelle Minéralogie (Paris) 121.174. Crystal from alluvial deposit.
16. Mogok, Burma. Brit. Mus. BM 1920,17. Crystal from alluvial deposit at a ruby mine (Spencer, 1920).
17. Mogok, Burma. Amer. Mus. Nat. History 34923. Crystal from alluvial deposit.
18. Sri Lanka Brit. Mus. BM 1945,39. Crystal from alluvial deposit.
19/20. Bournac, Haute-Loire, France. Mus. Nat. d'Histoire Naturelle Minéralogie (Paris) 129.7. From xenolith of garnet quartzofeldspathic gneiss in basaltic tuff (Caillère and Pobeguin, 1972). Analysis: Grew (1980); 0.24% Fe_2O_3 on a crystal by energy dispersive analysis.
21/22. From xenolith of quartzofeldspathic gneiss, Kilbourne Hole, New Mexico, U. S. A. Grew #76-5-24.

Table entries in weight percent. Analyses by electron microprobe-analysis, except:
*Energy dispersive spectroscopy under scanning electron microscope.

Kilbourne Hole ranges from 0.35 to 0.94 wt.% (6 samples), and at Bournac, 0.17 to 0.23 wt.% (5 samples). On the other hand, colorless and yellow sillimanite at Kilbourne Hole contain 0.99 and 1.82 wt.%, and colorless sillimanite at Bournac, 0.70 and 0.87 wt.%. Padovani and Carter (1977a) also report that the Fe_2O_3 content of blue sillimanite is less than that of colorless sillimanite at Kilbourne Hole. Moreover, at both localities, graphite is found only in those xenoliths in which the sillimanite contains less than 0.4 wt.% Fe_2O_3. Padovani and Carter (1977a) report the close association of graphite, blue sillimanite, and purple to blue rutile in the Kilbourne Hole xenoliths. Ilmenite is present in some xenoliths with blue sillimanite. Recalculated microprobe analysis (from stoichiometry) of two such ilmenites from Kilbourne Hole indicate Fe_2O_3 contents of 1 mole% or less (samples 76-5 and 76-5-9, Grew, 1977a), which is less than in ilmenite associated with yellow sillimanite (*e.g.*, Table 1, and Grew, 1980). These relations suggest that development of the blue color is associated with low Fe_2O_3 contents and may be promoted by a reducing environment.

The xenolithic sillimanites are typically chatoyant from fine acicular inclusions oriented parallel to [001], a feature noted in some crystals from Sri Lanka (Spencer, 1920). Such chatoyancy is not limited to these blue sillimanites. Some colorless sillimanite we have examined from the exposed granulite-facies terrain in Enderby Land, Antarctica, is also chatoyant and pale blue as a result of scattering by these fine inclusions. However, this sillimanite lacks the absorption spectra characteristic of the blue sillimanite descibed below.

The relative abundance of blue sillimanite in the xenoliths and its apparent absence in exposed metamorphic terrains suggests that interaction between the xenoliths and basalt host during their incorporation in the host or during transport to the earth's surface, or rapid quenching following transport may play a role in developing the blue color. These processes have evidently led to the nearby complete Al-Si disorder in associated K-feldspar (Grew, 1979). The alluvial blue sillimanite most probably is derived from nearby exposed granulite-facies terrains; the origin of this material remains an enigma.

Optical spectra

The pleochroic scheme for blue sillimanite is X and Y = colorless to pale yellow and Z = blue (see also Spencer, 1920; Winchell and Winchell, 1951). The absorption spectra of all blue samples are similar to one another, and are distinct from the spectra obtained of yellow and brown sillimanite. The pattern of a sillimanite from Sri Lanka (Ceylon) is representative of blue sillimanite (Fig. 9).

The prominent absorption features are two bands polarized $\|c$ (γ) centered at 595 and ~836 nm. There is little absorption in the α and β directions. Weak absorption features in the 350–500 nm region that correspond to the Fe^{3+} features in the spectra of yellow sillimanite are present in α, β, and γ. The intensities of these weak features do not correlate with the intensity of the two strong features. The intensities of the 595 and 836 nm features are correlated (Fig. 10) and consequentially are assumed to arise from the same source.

Chemical analyses of the blue sillimanites (Table 3) indicate that Fe and Ti are the major trace elements. The intensity of the 595 nm feature is not correlated with either the iron or the titanium content.

Relationship to blue kyanite

Several similarities between the spectra of blue kyanite and blue sillimanite are evident: (1) absorption bands occur at nearly the same wavelengths, (2) the lower energy band is about ⅓ as intense as the high energy band, and (3) both absorption bands are polarized along the octahedral chain axis. These similarities suggest that the blue color in both minerals has the same origin.

The origin of the blue color in kyanite has been addressed several times (White and White, 1967;

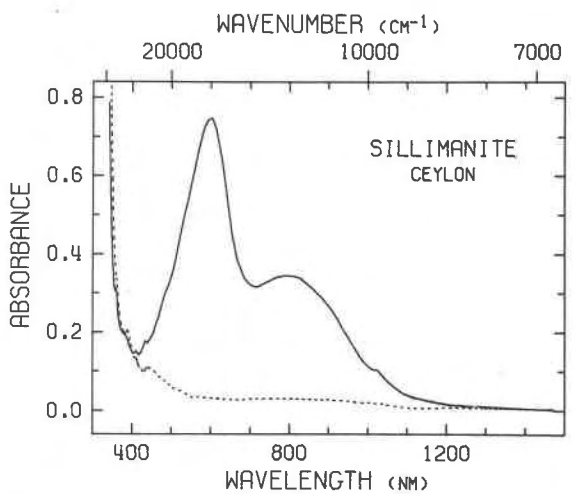

Fig. 9. Optical absorption spectrum of blue sillimanite (#18). Thickness = 6.0 mm; α = dots, γ = dash. The β-spectrum (not illustrated) is nearly identical to the α-spectrum.

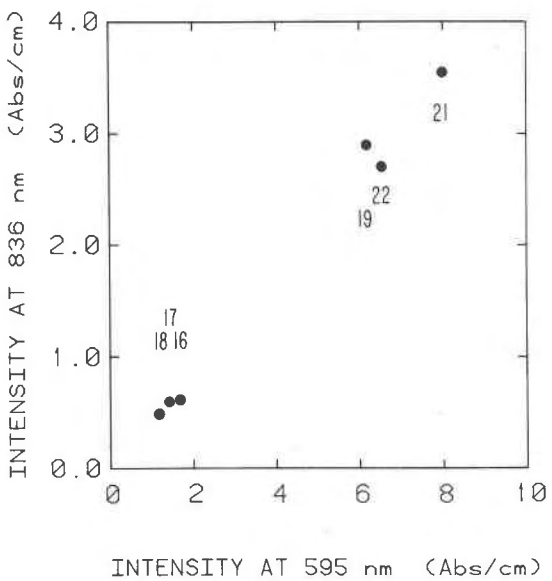

Fig. 10. Correlation of the 595 nm and 836 nm absorption bands of blue sillimanite. The numbers designating dots are sample numbers from Table 3.

Faye and Nickel, 1969; Faye, 1971; Smith and Strens, 1976; Parkin, *et al.*, 1977). All authors recognize the likelihood that intervalence charge transfer absorption is the process responsible for the color. Two broad, overlapping absorptions are prominent in the absorption spectrum of blue kyanite, one at ~600 nm and weaker one at ~850 nm. They are generally believed to arise from either Fe^{2+}–Ti^{4+} or Fe^{2+}–Fe^{3+} intervalence charge transfer.

Iron and titanium are present in blue sillimanite, but both are also present in yellow sillimanite. The color-producing mechanisms proposed for kyanite involving trace amounts of Fe^{2+} are also appropriate for blue sillimanite in view of its association with reducing environments. The amount of Fe^{2+} in sillimanite must be small because the characteristic pair of Fe^{2+} absorption bands has not been observed in the sillimanite spectrum. The details of the mechanism by which Fe^{2+} would produce the color are not established; it is not known whether the color-causing ions are in true solid solution or are associated the incipient exsolution of inclusions such as rutile.

Conclusions

Yellow and brown appear to be the characteristic colors of sillimanite in high-grade metamorphic rocks. Sillimanite contains a small amount of Fe_2O_3 (up to 1.8 wt.%) and Fe^{3+} is the primary cause of the color, as absorption increases with Fe_2O_3 content. A variety of experiments suggest that the Fe^{3+} occurs in both octahedral and tetrahedral sites. A few sillimanites contain a small amount of Cr^{3+} (up to 0.3 wt.% Cr_2O_3 in Antarctic sillimanite, Grew, in preparation) which contributes a green hue to the yellow in such samples.

Brown color in sillimanite appears to be related to incipient exsolution of iron-titanium oxides from sillimanite. It is restricted to samples relatively rich in Fe^{3+} ($\geq$1 wt.% Fe_2O_3) which generally originate from relatively oxidized rocks. Most brown sillimanite contains acicular inclusions of opaque or dark brown material, presumably an Fe or Fe–Ti oxide. In contrast to yellow sillimanite, the intensity of color does not increase proportionally to the Fe content.

Sillimanite from xenoliths of granulite and gneiss incorporated in basaltic rocks differs from the sillimanite of exposed high-grade terrains. In the only yellow xenolithic sample we had, the optical absorption intensity and Mössbauer spectrum are much weaker than those of a non-xenolithic sillimanite containing the equivalent amount of iron. Possibly the iron in the xenolithic sillimanite is distributed more evenly throughout the crystal than in the non-xenolithic sillimanite. This more even distribution may be related to the thermal history of the xenolithic samples. The xenoliths were heated to magmatic temperatures and rapidly quenched to the ambient temperature at the Earth's surface. K-feldspar in a xenolith at the same locality (Kilbourne Hole) has an unusually high degree of Al–Si disorder, one of the highest reported in the literature (Grew, 1979). This rapid quenching may have preserved the highly diffused Fe^{3+} distribution induced at high temperatures. In the sillimanite from exposed metamorphic terrains, less rapid cooling allowed the Fe^{3+} to migrate and cluster to a limited extent.

Xenolithic sillimanite containing less than 1 wt.% Fe_2O_3 is blue in some cases. Rapid quenching from high temperatures under reducing conditions (*i.e.*, low Fe_2O_3) may be instrumental in developing the blue color in sillimanite. However, this mechanism does not explain the blue color of alluvial gem quality sillimanite from Sri Lanka and Burma. Nor does it account for the related blue color in kyanite, the characteristic color of kyanite from exposed regionally metamorphosed terrains, which must have cooled slowly.

Acknowledgments

Grew thanks members of the 18th and 19th Soviet Antarctic Expeditions (1973–74) and of the 1977–78 and 1979–80 Australian National Antarctica Research Expeditions for providing logistic support for field work in Antarctica. Grew also thanks P. C. Grew for assistance in collecting xenoliths at Kilbourne Hole and Bournac.

We acknowledge the following people and institutions for their generosity in providing us with samples for this study: C. Frondel–Harvard University; J. S. White, Jr.—The U. S. National Museum (Smithsonian Institution); J. P. Fuller–The British Museum; J. Fabriès—The Muséum d'Histoire Naturelle (Minéralogie); G. E. Harlow–the American Museum of Natural History; U. Hålenius, E. R. Padovani and F. H. Pough. David Veblen provided electron microscopy results; K. Langer and R. G. Burns provided helpful discussion of our results.

This work was funded in part by National Science Foundation grants DPP 75-17390 and DPP 76-80957 to UCLA, and EAR 79-04801 to Caltech; electron microscopy studies were funded by grant EAR 81-15790 to Arizona State University.

References

Adams, F. D. and Graham, R. P. D. (1926) On some minerals from the ruby mining district of Mogok, Upper Burma. Transactions of the Royal Society Canada 20, 113–136.

Bank, H. (1974) Durchsichtiger farbloser bis bläulicher Sillimanit aus Kenya. Zeitschrift deutschen Gemmologischen Gesellschaft, 23, 281–282.

Bowen, G. T. (1824) Description and analysis of the sillimanite, a new mineral. American Journal of Science, 8, 113–118.

Burnham, C. W. (1963a) Refinement of the crystal structure of sillimanite. Zeitschrift für Kristallographie, 118, 127–148.

Burnham, C. W. (1963b) Refinement of the crystal structure of kyanite. Zeitschrift für Kristallographie, 118, 337–360.

Caillère, S., and Pobeguin, T. (1972) Sur la présence de sillimanite à Bournac (Haute-Loire). Bulletin de la Société française de Minéralogie et de Cristallographie, 95, 411.

Dana, E. S. (1920) Descriptive Mineralogy, John Wiley & Sons, New York.

Faye, G. H. (1969) The optical absorption spectrum of tetrahedrally bonded Fe^{3+} in orthoclase. Canadian Mineralogist, 10, 112–117.

Faye, G. H. (1971) On the optical spectra of di- and trivalent iron in corundum: a discussion. Canadian Mineralogist, 56, 344–348.

Faye, G. H. and Harris, D. C. (1969) On the origin of color and pleochroism in andalusite from Brazil. Canadian Mineralogist, 10, 47–56.

Faye, G. H. and Nickel, E. H. (1969) On the origin of color and pleochroism of kyanite, American Mineralogist, 10, 35–46.

Grew, E. S. (1976) Blue sillimanite (abstr.). Transactions of the American Geophysical Union, 57, 1019.

Grew, E. S. (1977a) Blue sillimanite and the origin of crustal xenoliths at Kilbourne Hole, New Mexico, and Bournac, Haute-Loire, France (abstr.). Extended Abstracts, contributed to the Second International Kimberlite Conference, Santa Fe, New Mexico, Oct. 3–7, 1977.

Grew, E. S. (1977b) First report of kyanite-sillimanite association in New Zealand (Note). New Zealand Journal of Geology and Geophysics, 20, 797–802.

Grew, E. S. (1979) Al–Si disorder of K-feldspar in crustal xenoliths at Kilbourne Hole, New Mexico. American Mineralogist, 64, 912–916.

Grew, E. S. (1980) Sillimanite and ilmenite from high-grade metamorphic rocks of Antarctica and other areas. Journal of Petrology, 21, 39–68.

Grew, E. S. (1981a) Granulite-facies metamorphism at Molodezhnaya Station, East Antarctica. Journal of Petrology, 22, 297–336.

Grew, E. S. (1981b) Surinamite, taaffeite, and beryllian sapphirine from pegmatites in granulite-facies rocks of Casey Bay, Enderby Land, Antarctica. American Mineralogist, 66, 1022–1033.

Grew, E. S. and Manton, W. I. (1979) Archean rocks in Antarctica: 2.5-billion-year uranium-lead ages of pegmatites in Enderby Land. Science, 206, 443–445.

Grew, E. S. and Rossman, G. R. (1976a) Iron in some Antarctic sillimanites (abstr.). Transactions of the American Geophysical Union, 57, 337.

Grew, E. S. and Rossman, G. R. (1976b) Color and iron in sillimanite (abstr.). Abstracts, 25th International Geological Congress, 2, 564–565.

Hålenius, U. (1979) State and location of iron in sillimanite. Neues Jahrbuch für Mineralogie Monatshefte, 165–174.

Hattori, H. (1967) Occurrence of sillimanite-garnet-biotite gneisses and their significance in metamorphic zoning in the South Island, New Zealand. New Zealand Journal of Geology and Geophysics, 10, 269–299.

Hutton, D. R. and Troup, G. J. (1964) Paramagnetic resonance of Fe^{3+} in kyanite. British Journal of Applied Physics, 15, 1493–1499.

Lehman, G. (1970) Ligand field and charge transfer spectra of Fe(III)–O complexes. Zeitschrift für Physikalische Chemie Neue Folge, 72, 279–297.

LeMarshall, J., Huton, D. R., Troup, G. J., and Thyer, J. R. W. (1971) Paramagnetic resonance study of Cr^{3+} and Fe^{3+} in sillimanite. Physics Status Solidi A., 769–773.

Leong, K. M. and Moore, J. M., Jr. (1972) Sapphirine-bearing rocks from Wilson Lake, Labrador. Canadian Mineralogist, 11, 777–790.

Leyreloup, A., Dupuy, C., and Andriambololona, R. (1977) Catazonal xenoliths in French Neogene rocks: constitution of the lower crust. 2. Chemical composition and consequences of the evolution of the French Massif Central Precambrian crust. Contributions to Mineralogy and Petrology 62, 238–300.

Morse, S. A. and Talley, J. H. (1971) Sapphirine reactions in deep-seated granulites near Wilson Lake, Central Labrador, Canada. Earth and Planetary Science Letters, 10, 325–328.

Overstreet, W. C. and Bell, H., III (1965) The crystalline rocks of South Carolina. U. S. Geological Survey Bulletin 1183.

Padovani, E. R. and Carter, J. L. (1973) Mineralogy and mineral chemistry of a suite of anhydrous, quartzo-feldspathic, garnet-bearing granulites from Kilbourne Hole maar, New Mexico (abstr.). Geological Society of America Abstracts with Programs, 5, 761–762.

Padovani, E. R. and Carter, J. L. (1974) Blue sillimanite in garnet granulite xenoliths from Kilbourne Hole, New Mexico (abstr.). Transactions of the American Geophysical Union, 55, 482.

Padvoani, E. R. and Carter, J. L. (1977a) Aspects of the deep crustal evolution beneath south central New Mexico. In J. G. Heacock, Ed., The Earth's Crust, p. 19–55. American Geophysical Union Geophysical Monograph 20.

Padovani, E. R. and Carter, J. L. (1977b) Non-equilibrium partial fusion due to decompression and thermal effects in crustal xenoliths. In H. B. J. Dick, Ed., Magma Genesis, p. 43–57. Oregon Department of Geology and Mineral Industries, Bulletin 96.

Parkin, K. M., Loeffler, B. M. and Burns, R. G. (1977) Mössbauer spectra of kyanite, aquamarine, and cordierite showing intervalence charge transfer. Physics and Chemistry of Minerals, 1, 301–311.

Rossman, G. R. (1975) Spectroscopic and magnetic studies of ferric iron hydroxy-sulfates: intensification of color in ferric iron clusters bridged by a single hydroxide ion. American Mineralogist, 60, 698–704.

Schairer, J. F. (1931) The minerals of Connecticut. Connecticut State Geological and Natural History Survey, Bulletin No. 51.

Smith, G. and Strens, R. G. J. (1976) Intervalence-transfer absorption in some silicate, oxide and phosphate minerals. In R. G. J. Strens, Ed., The Physics and Chemistry of Minerals and Rocks, p. 583–612. John Wiley & Sons, New York.

Spencer, L. J. (1920) Fibrolite (=sillimanite) as a gemstone from Burma and Ceylon. Mineralogical Magazine, 19, 107–112.

Thompson, J. B., Jr. and Norton, S. A. (1968) Paleozoic regional metamorphism in New England and adjacent areas. In E. Zen, W. S. White. J. B. Hadley and J. B. Thompson, Jr., Eds. Studies of Appalachian Geology Northern and Maritime, p. 319–327, John Wiley and Sons, New York.

Vrána, S. (1979) A polymetamorphic assemblage of grandidierite, kornerupine, Ti-rich dumortierite, tourmaline, sillimanite and garnet. Neues Jahrbuch für Mineralogie Monatshefte 1979, 22–33.

White, E. W. and White, W. B. (1967) Electron microprobe and optical absorption study of colored kyanites. Science, 158, 915–917.

Wignall, J. W. G. (1966) Mössbauer line broadening in trivalent iron compounds. Journal of Chemical Physics, 44, 2462–2467.

Wilkins, R. W. T. and Sabine, W. (1973) Water content of some nominally anhydrous silicates. American Mineralogist, 58, 508–516.

Winchell, A. N. and Winchell, H. (1951) Elements of Optical Mineralogy. An introduction to Microscopic Petrography. Part II. Descriptions of Minerals. Fourth Edition, John Wiley and Sons, New York.

Manuscript received, January 6, 1982;
accepted for publication, March 18, 1982.